Effect of Piston-Slipper Assembly Mass Difference on the Cylinder Block Tilt in a High-Speed Electro-Hydrostatic Actuator Pump of Aircraft

Junhui Zhang[1,#], Qun Chao[1], Bing Xu[1], Min Pan[2], Yuan Chen[1], Qiannan Wang[1], and Ying Li[1]

1 State Key Laboratory of Fluid Power and Mechatronic Systems, Zhejiang University, No. 38 Zheda Road, Hangzhou, 310027, China
2 Department of Mechanical Engineering, University of Bath, Bath BA2 7AY, Avon, United Kingdom
Corresponding Author / E-mail: benzjh@zju.edu.cn, TEL: +86-571-87952505, FAX: +86-571-87952507

KEYWORDS: Piston-slipper assembly, Mass difference, Cylinder block tilt, Electro-hydrostatic actuator pump

When manufacturing axial piston pumps, mass difference of piston-slipper assembly is inevitable because of manufacturing precision limits. Small mass difference may not cause problems when the pump operates at low speeds, while it cannot be ignored at high speeds. One problem related to high speed is the cylinder block tilt resulting from the inertial effect of piston-slipper assembly. Recently, the speed of electro-hydrostatic actuator (EHA) pump in aircraft can reach more than 10,000 rpm. Therefore, mass difference of piston-slipper assembly should be taken into account in future EHA pump design. The main purpose of this paper is to investigate the effect of the mass difference of piston-slipper assembly on the cylinder block tilt in a high-speed EHA pump. A detailed set of relevant equations is developed to establish the relationship between the mass difference of piston-slipper assembly and cylinder block tilting moment. It is found that a tighter control over the mass difference of piston-slipper assembly should be guaranteed when it comes to high-speed EHA pumps.

Manuscript received: September XX, 201X / Accepted: September XX, 201X

1. Introduction

The power-by-wire (PBW) systems have been successfully applied to more eclectic aircrafts (MEA) recently, replacing the conventional flight-by-wire systems which are based upon central hydraulic systems. MEA provides both aircraft's manufacturers and operators considerable benefit, such as weight saving, high efficiency and improved safety.[1-4] EHA plays an important role in the development of PBW technology providing power for primary flight control surfaces. A typical EHA system is mainly comprised of a fixed displacement axial piston pump, a servomotor and a hydraulic cylinder, forming a closed circuit. In the EHA system, the velocity and direction of the hydraulic actuator are controlled by the fluid flow from an electric motor driven hydraulic pump which is called EHA pump.[5]

Figure 1 shows a typical axial piston pump applied to the EHA system. The pump has a cylindrical block containing several pistons about its centerline at equal angular intervals. Each slipper connects itself with the piston via a ball-joint and keeps reasonable contact with the swash plate utilizing the retainer. On the one hand, the compressed cylinder block spring pushes the cylinder block against the fixed valve plate. On the other hand, the compressed cylinder block spring transfers its force to the retainer using several pins and a spherical cup. When the pump operates, the cylinder block is driven by the shaft using the spline mechanism. When the cylinder block rotates about the axis of the shaft, each slipper reciprocates within the cylinder bore due to the retainer and angled swash plate. The reciprocating motion of slippers causes the suction and discharge of the working fluid through openings in the valve plate. The pump displacement and speed determine the volumetric flow of the pump, especially when the pump is a fixed displacement pump, the volumetric flow of the pump is only determined by the pump speed. Higher pump speed can provide larger volumetric flow for the hydraulic system.

As the pump operates, three main necessary lubricating interfaces are forming between movable parts: the slipper/swash plate interface, the piston/cylinder block interface, and the cylinder block/ valve plate interface. These interfaces act as bearing and sealing functions, which significantly influence volumetric losses of the pump. The overall pump leakage is mainly determined by individual leakage sources through these three lubricating interfaces.

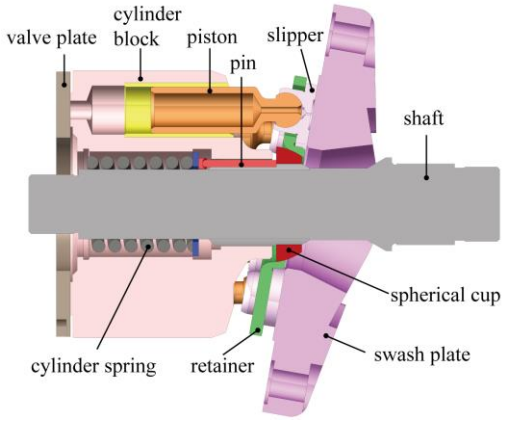

Fig. 1 The general configuration of an axial piston pump

For the aim of higher power density, the continuing development of EHA has put forward higher demand upon EHA pumps for higher rotating speed. Generally, an EHA pump is characterized as small displacement as well as high speed since this combination can offer large flow to produce sufficient velocity for the hydraulic cylinder by a more compact structure. At present, the electrically-driven mini-pumps developed by Messier-Bugatti, as part of EHA system driving the backup flight control, can be driven at rotating speed of up to 15,000 rpm. Also, similar EHA pumps provided for F-35 by Parker can operate at 20,000 rpm. However, there are some challenges that must be considered when designing high-speed EHA pumps.

The first problem associated with the high speed is high pressure pulsation. Edge and Darling[6] conducted theoretical and experimental studies of the cylinder block pressure in an axial piston pump and found that undershooting or overshooting pressure in the cylinder block increased almost linearly with the pump speed. Also, similar research was carried out by Carsten et al.[7]

The second problem pertaining to high rotating speed is cavitation. Harris et al.[8] developed cavitation and air-release models, according to which cavitation is likely to take place in high-speed conditions. Yamaguchi and Takabe[9] examined the cavitation experimentally in an axial piston pump and discovered that higher rational speed might need higher suction tank pressure. Manring[10] obtained the expression for speed limitation derived from Bernoulli equation and pointed out that the pump rational speed could be further improved when the intake pressure was increased.

The third problem of high rotating speed is concerned with power losses due to high-speed rotating elements in an axial piston machine. The power losses mainly result from mechanical friction due to metallic contact of sliding surfaces and churning losses due to rotating elements in the fluid-filled pump case. Hong et al.[11-13] pointed out that the EHA pump usually experienced mixed friction and the friction loss was mainly from the valve plate and input shaft bearing in a bent-axis type piston pump for the EHA at high speeds up to 10,000 rpm. Lee et al.[14] investigated the effects of duplex treatment on the surface properties of EHA pump parts by a high-speed disk-to-disk type wear test and found that a duplex treatment was effective in reducing wear rate. Besides, special attentions shall be given to churning losses that contribute significantly to power losses within high-speed pumps or motors.[15-17]

The last problem caused by high rotating speed is the instability of rotating parts in the high-speed piston pump. Especially, slippers and cylinder block tend to suffer from tilting moments because of the large translational inertial and centrifugal forces of piston-slipper assemblies in high-speed conditions.[10,18-20] Unfortunately, such tilting moments often result in slipper tilting away from the swash plate and cylinder block tilting away from the valve plate.[21-24] These tilting motions will lead to a wedge-shaped oil film between movable parts and thus increased leakage.

It can be seen from the last problem that the piston-slipper assembly inertia has a significant influence on pump performance. Conventional dynamics analysis for rotating parts of the pump is based on the assumption that all piston-slipper assemblies have the same mass. However, it is impossible for piston-slipper assemblies to remain the same mass due to limited manufacture precision.

Table 1 gives the actual mass of each piston-slipper assembly from commercial axial piston pumps. All of the data presented in this table are obtained from actual measurements. It should be noted that the max absolute mass error is equal to the maximum absolute difference value between the individual piston-slipper mass and piston-slipper average mass, and the max relative mass error is defined as the ratio of max absolute mass error to average mass.

Table 1 (a) Max. displacement and max. rotating speed of the actual machinery

Pump number	1	2	3
Max. displacement (mL/r)	60	45	28
Max. speed (rpm)	3000	3250	3600

Table 1 (b) Individual piston-slipper mass of the actual machinery

Piston-slipper number	Pump 1	Pump 2	Pump 3
1	119.55	103.63	70.23
2	118.93	102.89	70.10
3	119.42	103.17	70.34
4	118.87	103.43	70.13
5	119.56	102.99	70.02
6	118.93	103.57	69.97
7	118.72	102.73	69.83
8	119.42	103.04	70.32
9	119.05	103.23	70.42
Average mass (g)	119.16	103.19	70.15
Max. absolute mass error (g)	0.44	0.46	0.32
Max. relative mass error	0.37 %	0.44 %	0.46 %

The above mass difference of piston-slipper assembly may be a negligible factor when carrying out the dynamics analysis in low-speed conditions, but it cannot be ignored at high pump speeds. The small mass difference of piston-slipper assembly can produce large inertia force when the pump operates at high speeds, which may cause significant tilting inertia moment on the cylinder block.

Although much research has been conducted in high-speed problems, little information is available from the manufacture precision point of view. In this paper, motion equations of the piston-slipper assembly are given by using the vector analysis in which the piston-slipper mass difference is considered, also the rotating vector

method is applied for evaluating the effect of the piston-slipper assembly mass difference on the cylinder block tilt. Finally, the explicit theoretical expression for cylinder block tilting moment caused by the piston-slipper mass difference is proposed, according to which a tighter control over the mass difference of piston-slipper assemblies should be achieved in high-speed EHA pumps.

2. Mathematical model

From the literature[10] it is noticed that the cylinder block tilt is caused by the moments acting on the cylinder block by the centrifugal forces of all piston-slipper assemblies. In the present work, the translational inertia forces of piston-slipper assemblies will be considered as well as the centrifugal forces. Additionally, for any individual piston-slipper assembly, its mass is variable rather than constant.

Figure 2 shows a simplified cross-sectional view of a schematic diagram of an axial piston pump that mainly consists of the valve plate, cylinder block, piston, slipper, swash plate and other components not shown here for brevity. In Fig. 2, the *XYZ* system is fixed in an inertial frame and the *xyz* system attached to the cylinder block rotates relative to the *XYZ* system.

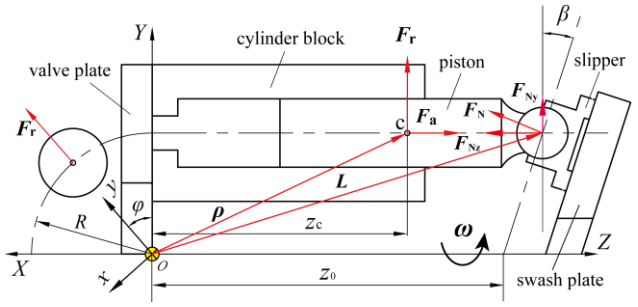

Fig. 2 Simplified cross-sectional view of the axial piston pump

Suppose that $\boldsymbol{\rho}$ is the position vector of the centroid of the piston-slipper assembly relative to the origin of the *XYZ* system. Then the vector expression for the absolute acceleration of the centroid of piston-slipper assembly is[25]

$$\boldsymbol{a}=\dot{\boldsymbol{\omega}}\times\boldsymbol{\rho}_n+\boldsymbol{\omega}\times\left(\boldsymbol{\omega}\times\boldsymbol{\rho}_n\right)+\left(\ddot{\boldsymbol{\rho}}_n\right)_{\mathrm{r}}+2\boldsymbol{\omega}\times\left(\dot{\boldsymbol{\rho}}_n\right)_{\mathrm{r}} \tag{1}$$

where $\boldsymbol{\omega}$ is the absolute angular speed of the cylinder block in the negative *Z*-direction that takes a constant value, $\dot{\boldsymbol{\omega}}$ is the absolute angular acceleration of the cylinder block, $\boldsymbol{\rho}_n$ is the position vector of the centroid of the *n*th piston-slipper assembly relative to the *xyz* system, $(\dot{\boldsymbol{\rho}}_n)_{\mathrm{r}}$ and $(\ddot{\boldsymbol{\rho}}_n)_{\mathrm{r}}$ are the velocity vector and acceleration vector of the centroid of the *n*th piston-slipper relative to the *xyz* system.

Before evaluating each of the terms in Eq. (1), we note that[26]

$$\boldsymbol{\omega}=-\omega\boldsymbol{k} \tag{2}$$

$$\left(\boldsymbol{\rho}_n\right)_{\mathrm{r}}=-R\tan\beta\left(1-\cos\varphi_n\right)\boldsymbol{k} \tag{3}$$

$$\boldsymbol{\rho}_n=R\sin\varphi_n\boldsymbol{i}+R\cos\varphi_n\boldsymbol{j}+\left(z_{\mathrm{c}}+\left(\rho_n\right)_{\mathrm{r}}\right)\boldsymbol{k} \tag{4}$$

where $\boldsymbol{i}$, $\boldsymbol{j}$ and $\boldsymbol{k}$ are the unit vectors in the *X*-direction, *Y*-direction and *Z*-direction respectively in the *XYZ* system, ω is the magnitude of cylinder block angular speed $\boldsymbol{\omega}$, *R* is the pitch circle radius of piston bores, β is the swash plate angle, z_{c} is the initial position of the centroid of the first piston-slipper assembly, and φ_n is the angular position of the *n*th piston. If $\varphi_1 = 0$ when the bottom dead center (BDC) is chosen as the position for the derivation of kinematic parameters, then

$$\varphi_n=\omega t+\left(n-1\right)\alpha \tag{5}$$

where α is the angular interval between two contiguous pistons about the z-axis.

Now solving for the absolute acceleration of the centroid of the piston-slipper assembly from Eqs. (1) to (5), we obtain

$$\boldsymbol{a}_n=-\omega^2R\left(\sin\varphi_n\boldsymbol{i}+\cos\varphi_n\boldsymbol{j}\right)-\omega^2R\tan\beta\cos\varphi_n\boldsymbol{k} \tag{6}$$

in which the first term on the right side represents the centrifugal acceleration arising from the rotating motion along with the cylinder block, and the second term represents the translational acceleration resulting from the reciprocating motion during discharge stoke and suction stroke.

Applying D'Alembert's principle, the centrifugal acceleration will generate radial inertial force $\boldsymbol{F}_{\mathbf{r}}$, and the translational acceleration will generate additional lateral inertial force $\boldsymbol{F}_{\mathbf{Ny}}$. These two types of inertia forces may lead to cylinder block tilting from the valve plate. Thus, taking tilting moment about origin, we obtain

$$\begin{aligned}\boldsymbol{M}_{\mathbf{T}}=&\sum_{n=1}^{N}\left[\boldsymbol{\rho}_n\times\left(\omega^2Rm_n\sin\varphi_n\boldsymbol{i}+\omega^2Rm_n\cos\varphi_n\boldsymbol{j}\right)\right]\\&+\sum_{n=1}^{N}\left(\boldsymbol{L}_n\times\omega^2R\tan^2\beta m_n\cos\varphi_n\boldsymbol{j}\right)\end{aligned} \tag{7}$$

where m_n is the *n*th piston-slipper mass, *N* is the total number of pistons and $\boldsymbol{L}_n$ is the moment arm of the *n*th inertia force generated by the translational acceleration. It is noted that both $\boldsymbol{\rho}_n$ and $\boldsymbol{L}_n$ are vectors that are measured relative to the *XYZ* system. From Fig. 2, $\boldsymbol{L}_n$ is given by

$$\boldsymbol{L}_n=R\sin\varphi_n\boldsymbol{i}+R\cos\varphi_n\boldsymbol{j}+\left(z_0+R\tan\beta\cos\varphi_n\right)\boldsymbol{k} \tag{8}$$

where z_0 is the location of the intersection between the plane of all piston-slipper ball joints and the centerline of the shaft.

Substituting the results of Eqs. (4) and (8) into Eq. (7), we may obtain the tilting moment acting on the cylinder block.

$$\begin{aligned}\boldsymbol{M}_{\mathbf{T}}=&-\omega^2R\left[K_1\sum_{n=1}^{N}m_n\cos\varphi_n+K_2\sum_{n=1}^{N}m_n\cos\left(2\varphi_n\right)\right]\boldsymbol{i}\\&+\omega^2R\left[K_3\sum_{n=1}^{N}m_n\sin\varphi_n+K_4\sum_{n=1}^{N}m_n\sin\left(2\varphi_n\right)\right]\boldsymbol{j}\end{aligned} \tag{9}$$

where

$$K_1=z_{\mathrm{c}}-R\tan\beta+z_0\tan^2\beta \tag{10}$$

$$K_2 = \frac{1}{2} R \tan\beta \sec^2\beta \tag{11}$$

$$K_3 = z_c - R\tan\beta \tag{12}$$

$$K_4 = \frac{1}{2} R \tan\beta \tag{13}$$

Previous studies usually assumed that individual piston-slipper assemblies were identical in mass. Namely, each m_n was assumed to be constant. Therefore, the summations of the trigonometric series associated with K_1, K_3, and K_4 in Eq. (9) would be equal to zero due to mathematical symmetry. The specific assumption may be acceptable for the case of not very high pump speed because the mass deviation of piston-slipper assembly due to actual manufacturing errors may not cause significant cylinder block imbalance. However, the EHA pump applied to the electro-hydrostatic actuator is characterized as high speed more than 10,000 rpm, even a very small mass deviation of piston-slipper assembly is likely to give rise to large cylinder block tilting moment and thus cylinder block tilting from the valve plate.

Let us consider that the actual nth piston-slipper mass m_n deviates away from the nominal mass m_m by Δm_n. It is noted that the nominal mass m_m is equivalent to the average mass of all piston-slipper assemblies. Then the new expression for the cylinder block tilting moment derived from Eq. (9) is

$$\begin{aligned}\boldsymbol{M}_T = &-\omega^2 R\left[\begin{array}{l} K_1\sum_{n=1}^{N}\left(m_m+\Delta m_n\right)\cos\varphi_n \\ +K_2\sum_{n=1}^{N}\left(m_m+\Delta m_n\right)\cos\left(2\varphi_n\right)\end{array}\right]\boldsymbol{i} \\ &+\omega^2 R\left[\begin{array}{l} K_3\sum_{n=1}^{N}\left(m_m+\Delta m_n\right)\sin\varphi_n \\ +K_4\sum_{n=1}^{N}\left(m_m+\Delta m_n\right)\sin\left(2\varphi_n\right)\end{array}\right]\boldsymbol{j}\end{aligned} \tag{14}$$

Subtracting Eq. (9) from Eq. (14) after letting $m_n = m_m$ in Eq. (9) yields the additional cylinder block tilting moment due to the piston-slipper mass errors.

$$\begin{aligned}\Delta\boldsymbol{M}_T = &-\omega^2 R\left[K_1\sum_{n=1}^{N}\Delta m_n\cos\varphi_n + K_2\sum_{n=1}^{N}\Delta m_n\cos\left(2\varphi_n\right)\right]\boldsymbol{i} \\ &+\omega^2 R\left[K_3\sum_{n=1}^{N}\Delta m_n\sin\varphi_n + K_4\sum_{n=1}^{N}\Delta m_n\sin\left(2\varphi_n\right)\right]\boldsymbol{j}\end{aligned} \tag{15}$$

Considering $K_1 \approx K_3$ and $K_2 \approx K_4$ due to the small value of β, Eq. (15) can be further simplified as follows:

$$\begin{aligned}\Delta\boldsymbol{M}_T = &-\omega^2 R\left[K_1\sum_{n=1}^{N}\Delta m_n\cos\varphi_n + K_2\sum_{n=1}^{N}\Delta m_n\cos 2\varphi_n\right]\boldsymbol{i} \\ &+\omega^2 R\left[K_1\sum_{n=1}^{N}\Delta m_n\sin\varphi_n + K_2\sum_{n=1}^{N}\Delta m_n\sin 2\varphi_n\right]\boldsymbol{j}\end{aligned} \tag{16}$$

3. Analytical results and discussion

It can be seen from Eq. (16) that the mass difference of piston-slipper assembly will produce tilting moment components in the X and Y directions, as shown in Fig. 3. These two components of tilting moment contribute to cylinder block tilting away from the fixed valve plate about the X- and Y-axis during operation. One should note that the gap within the cylinder block/valve plate interface has been exaggerated for illustration purpose. The actual gap height is usually on the order of microns. Once the cylinder block tilt occurs, the wedge-shaped oil film probably forms between the cylinder block and valve plate, which may cause dramatically increased leakage flow.

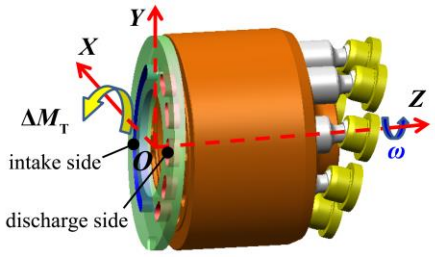

(a) Cylinder block tilt about X-axis

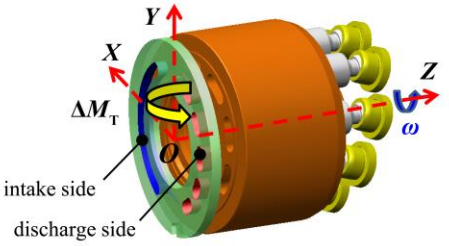

(b) Cylinder block tilt about Y-axis

Fig. 3 Cylinder block tilt by the additional tilting moment due to mass difference of piston-slipper assembly

It is a usual practice in the case of the piston-slipper assembly to limit its mass deviation during the design phase. For the case of axial piston pumps applied to construction machinery, the piston-slipper mass deviation from its nominal value is usually maintained within ±1 g according to experience. It must be emphasized, however, that the above empirical value is based upon normal speed lower than 4000 rpm in most cases. The EHA pump applied to EHA system usually operates at a high rotating speed more than 10,000 rpm, which is likely to trigger the cylinder block tilt. Therefore, a stricter limit on the piston-slipper mass deviation should be put forward for the EHA pump.

Applying Eq. (16), the additional tilting moment of cylinder block can be evaluated to investigate the effect of non-uniform piston-slipper mass on the cylinder block tilt. On the other hand, if we give insight into Eq. (16) from the mathematical point of view, then the additional tilting moment of cylinder block can be considered as consisting of one additional tilting moment $\Delta\boldsymbol{M}_{T1}$ and another one $\Delta\boldsymbol{M}_{T2}$.

$$\Delta \boldsymbol{M}_{\mathrm{T}} = \Delta \boldsymbol{M}_{\mathrm{T1}} + \Delta \boldsymbol{M}_{\mathrm{T2}} \tag{17}$$

$$\Delta \boldsymbol{M}_{\mathrm{T1}} = K_1 \omega^2 R \left[\sum_{n=1}^{N} \Delta m_n \left(-\cos \varphi_n \boldsymbol{i} + \sin \varphi_n \boldsymbol{j} \right) \right] \tag{18}$$

$$\Delta \boldsymbol{M}_{\mathrm{T2}} = K_2 \omega^2 R \left[\sum_{n=1}^{N} \Delta m_n \left(-\cos 2\varphi_n \boldsymbol{i} + \sin 2\varphi_n \boldsymbol{j} \right) \right] \tag{19}$$

Assume that the piston-slipper mass deviation Δm_n varies from -Δm to Δm. To calculate the maximum and minimum of Eqs. (18) and (19), the rotating vector method will be introduced in the following discussion. Traditionally, the total number of pistons N within an axial piston pump is 7, 9 or 11 for a low flow rate pulsation. Without any loss of generality, N is set equal to 9 for the investigated EHA pump.

Fig. 4 shows the rotating vector method for calculating the maximum of $\Delta \boldsymbol{M}_{\mathrm{T1}}$ using an indicator diagram. One can observe that each vector arrow icon represents the corresponding trigonometric term involved in the summation of trigonometric series in Eq. (18). Also, the angle between two adjacent vector arrows is α when Δm_n is a positive value, and the angle is π-α when Δm_n is a negative value. Then the maximum of $\Delta \boldsymbol{M}_{\mathrm{T1}}$ is indicated by $\overrightarrow{OO_1}$.

$$\left| \Delta \boldsymbol{M}_{\mathrm{T1}} \right|_{\max} = K_1 \omega^2 R \frac{\Delta \mathrm{m}}{2 \sin \dfrac{\alpha}{4}} \tag{20}$$

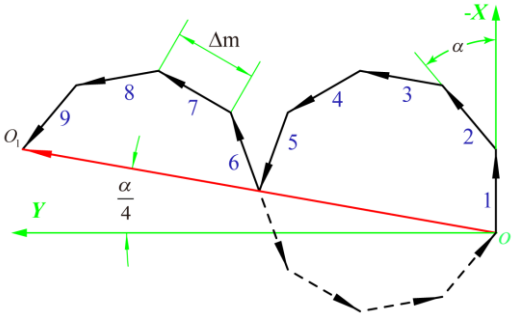

Fig. 4 Indicator diagram for the maximum of $\Delta \boldsymbol{M}_{\mathrm{T1}}$ ($\varphi_1 = 0°$)

In a similar manner, we could obtain the maximum of $\Delta \boldsymbol{M}_{\mathrm{T2}}$, as illustrated in Fig. 5.

$$\left| \Delta \boldsymbol{M}_{\mathrm{T2}} \right|_{\max} = K_2 \omega^2 R \frac{4\left(\sin 2\alpha + \sin 3\alpha \right) \Delta \mathrm{m}}{\cos \dfrac{\alpha}{4}} \tag{21}$$

Again looking at Fig. 4 and Fig. 5, it is found that when all piston-slipper assemblies have the same mass deviation, both magnitudes of $\Delta \boldsymbol{M}_{\mathrm{T1}}$ and $\Delta \boldsymbol{M}_{\mathrm{T2}}$ turn out to be zero, as indicated by the dotted vector arrows. Additionally, another point to keep in mind is that both $\Delta \boldsymbol{M}_{\mathrm{T1}}$ and $\Delta \boldsymbol{M}_{\mathrm{T2}}$ cannot achieve their possible maximum in the same manner even if both of their resultant vectors have the same direction. This implies that both $\Delta \boldsymbol{M}_{\mathrm{T1}}$ and $\Delta \boldsymbol{M}_{\mathrm{T2}}$ cannot achieve their possible maximum simultaneously.

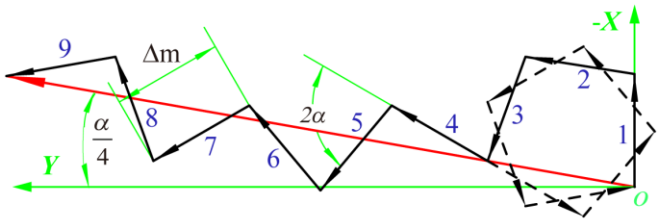

Fig. 5 Indicator diagram for maximum magnitude of $\Delta \boldsymbol{M}_{\mathrm{T2}}$ ($\varphi_1 = 0°$)

To evaluate the contribution of the piston-slipper assembly mass difference on the cylinder block tilt, it is required to introduce the traditional tilting moment acting on the cylinder block due to the pressure difference between the discharge side and suction side.[27-31] The mean value of the above traditional tilting moment can be expressed as[32]

$$M_{\mathrm{mean}} = \frac{2p}{9} \left[\frac{R_4^3 - R_3^3}{\ln\left(R_4 / R_3 \right)} - \frac{R_2^3 - R_1^3}{\ln\left(R_2 / R_1 \right)} \right] \cos \frac{\alpha - \alpha_1}{2} \cos \frac{\alpha}{4} \tag{22}$$

where p is the discharge pressure, R_1 and R_2 are the inside and outside radius of the inner region of the sealing land on the cylinder block, R_3 and R_4 are the inside and outside radius of the outer region of the sealing land on the cylinder block, and α_1 is the circumferential angle of kidney pattern of the cylinder block, as shown in Fig. 6.

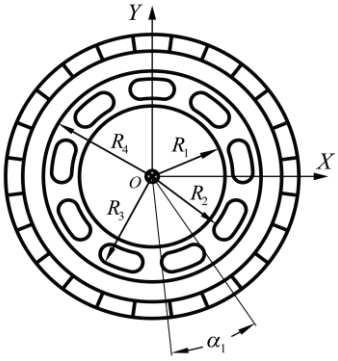

Fig. 6 A schematic of the cylinder block bottom sealing face

Comparing the magnitude of the additional tilting moments $\Delta \boldsymbol{M}_{\mathrm{T1}}$ and $\Delta \boldsymbol{M}_{\mathrm{T2}}$ with the traditional tilting moment M_{mean} may provide a better understanding of the influence of the piston-slipper mass difference. Fig. 7 and Fig. 8 show an example of calculations of the additional tilting moments $\Delta \boldsymbol{M}_{\mathrm{T1}}$ and $\Delta \boldsymbol{M}_{\mathrm{T2}}$ for a range of piston-slipper mass deviations. From the results shown in Figs. 7 and Fig. 8, it can be seen that the non-uniform piston-slipper mass has a significant impact on the additional tilting moment acting on the cylinder block at low pressures and high rotating speeds. The possible maximum of $\Delta \boldsymbol{M}_{\mathrm{T1}}$ can reach up to 53% of M_{mean} at 2 MPa and 20,000 rpm even though the mass deviation of each piston-slipper assembly is only 0.5 g or -0.5 g. Moreover, the magnitude of additional tilting moment $\Delta \boldsymbol{M}_{\mathrm{T1}}$ is overwhelmingly greater than that of $\Delta \boldsymbol{M}_{\mathrm{T2}}$.

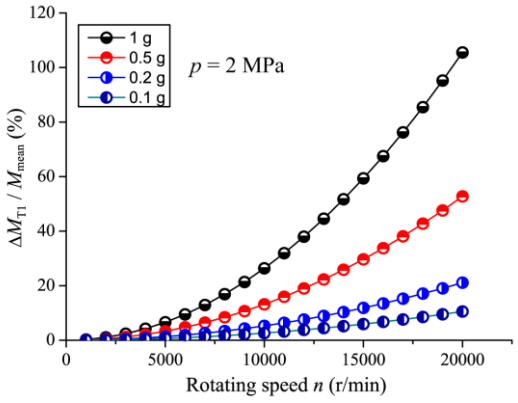

Fig. 7 Results for the additional tilting moment, ΔM_{T1}, for a range of piston-slipper mass deviations

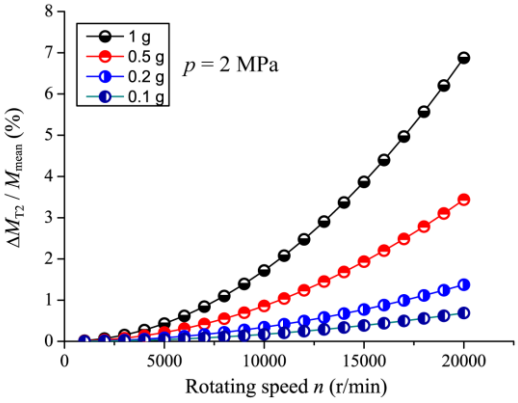

Fig. 8 Results for the additional tilting moment, ΔM_{T2}, for a range of piston-slipper mass deviations

The low-pressure and high-speed conditions are common for the EHA pump for the purpose of power saving.[33] Therefore, it is of importance to recognize that the individual piston-slipper assembly mass must keep more consistent with each other on the basis of the above analysis. If it is assumed that the magnitude of total additional tilting moments should be maintained below 10% of M_{mean} for the investigated EHA pump at 10,000 rpm, then it is recommended to limit the piston-slipper mass deviation Δm to be less than 0.2 g. Furtherly, if the investigated EHA pump operates at 20,000 rpm, then the Δm is recommended to be less than 0.1 g.

4. Experimental Verification

The aim of the experimental study is to verify the influence of the piston-slipper assembly mass difference on the cylinder block tilt. As stated previously, the cylinder block tilt may give rise to a wedge-shaped oil film within the cylinder block/valve plate interface, which consequently brings about an increase in leakage within this interface. As a result, the overall leakage of the pump will increase accordingly.

It is indeed a meaningful attempt to establish the relationship between the piston-slipper assembly mass difference and the leakage increase. However, it is not yet possible to calculate the complicated additional leakage only because of the piston-slipper assembly mass difference. On the other hand, it is difficult to directly measure the leakage flow between the cylinder block and valve plate. In order to get around this dilemma, we alternatively choose to investigate the overall leakage of the pump and qualitatively analyze the effect of the piston-slipper assembly mass difference on the cylinder block tilt. It is assumed that the leakage change from the cylinder block/valve plate can be reflected by the overall leakage change of the pump.

In order to measure the overall leakage of the high-speed EHA pump prototype, which was independently developed by State Key Laboratory of Fluid Power and Mechatronic Systems, Zhejiang University, a test rig presented in Fig. 9 was built up which was allowed to provide rotating speeds more than 10,000 rpm. The EHA pump prototype with a fixed displacement of 2 mL/r had a maximum pressure of 28 MPa and a maximum speed of 10,000 rpm.

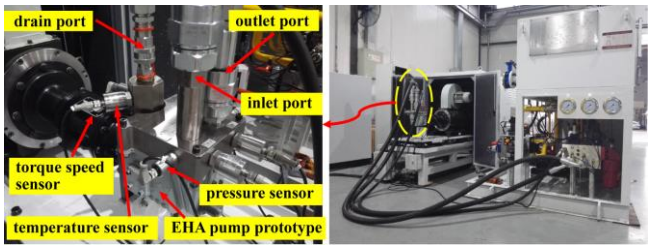

Fig. 9 Photograph of the test rig for the investigated EHA pump

Two groups (A and B) of piston-slipper assemblies were selected to be assembled into the EHA pump prototype. The mass of individual piston-slipper assemblies was measured using high-accuracy electronic scales, and one of the actual piston-slipper assemblies is shown in Fig. 10.

Fig. 10 Photograph of one individual piston-slipper assembly of the investigated EHA pump prototype

Table 2 lists the actual mass of each piston-slipper assembly used to be assembled into the investigated EHA pump prototype. It can be seen from Table 2 that these two groups have the same piston-slipper assembly mass from number 1 to number 8 except number 9. Besides, it is important to notice that these piston-slipper assemblies of each group were nested within the cylinder block in order of decreasing mass. This specific arrangement was to make it more convenient to compare the EHA pump prototype performance with different piston-slipper assembly mass deviations.

It is easy to obtain each piston-slipper assembly mass deviation by subtracting the average mass from the individual mass. Then we can calculate the additional cylinder block tilting moments due to the piston-slipper mass difference using Eqs. (18) and (19).

Table 2 Individual piston-slipper mass of the EHA pump prototype

Piston-slipper number	Group A	Group B
1	16.514	16.514
2	16.511	16.511
3	16.506	16.506
4	16.504	16.504
5	16.483	16.483
6	16.481	16.481
7	16.479	16.479
8	16.475	16.475
9	16.470	15.976
Average mass (g)	16.491	16.437
Max. absolute mass error (g)	0.023	0.461
Max. relative mass error	0.14%	28%

Figure 11 gives a graphical example of the actual additional tilting moment ΔM_{T1} acting on the cylinder block. The additional tilting moment, ΔM_{T2}, is not shown here since its magnitude can be negligible when compared with ΔM_{T1}.

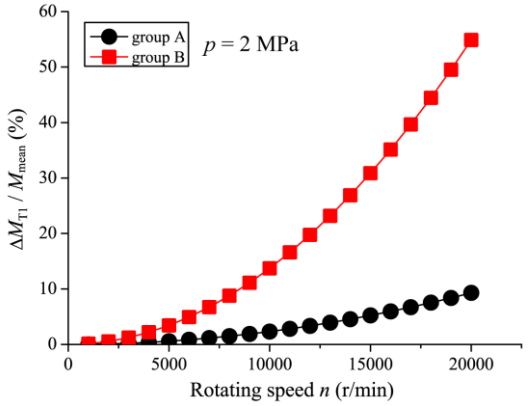

Fig. 11 Calculated additional cylinder block tilting moment ΔM_{T1}

Comparing the calculated results between group A and group B shown in Fig. 11, it can be found that the additional tilting moment acting on the cylinder block for group B is obviously larger than that for group A, especially at high rotating speeds. This is an expected result given that the non-uniformity degree of mass distribution for group B is larger than that for group A as shown in Table 2. Therefore the non-uniformity degree of mass distribution cannot be ignored when the EHA pump operates at high speeds since the cylinder block tilting effect increases quadratically with its rotating speeds.

Fig. 12 shows the trend of the measured overall leakage of the EHA pump prototype with increased rotating speed for group A and group B. These two groups of experiments were carried out at the same discharge pressure of 2 MPa, and the inlet oil temperature was maintained at (32±0.5)℃ in order to eliminate the influence of these two operating parameters on the pump leakage as far as possible.

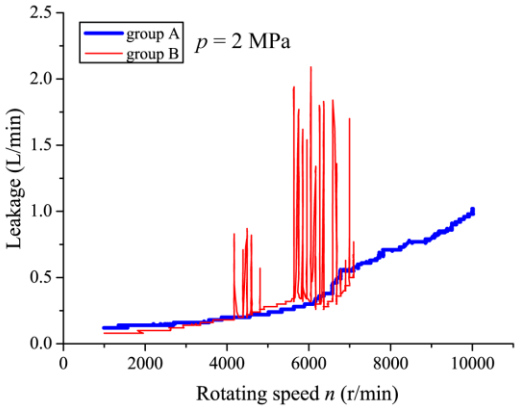

Fig. 12 Measured overall leakage of the EHA pump prototype

It is no surprise that there is little difference of the measured overall leakage between group A and group B when the EHA pump prototype operates at low rotating speeds (i.e., lower than 4000 rpm). This is due to the fact that the magnitude of the additional cylinder block tilting moment is rather small at low speeds, so that the cylinder block balance is less likely to be disturbed. At this time, the gap height between the cylinder block and valve plate is not significantly affected by the small tilting moment. However, when the rotating speed continues to rise, the additional tilting moment acting on the cylinder block can no longer be ignored. It can be seen from Fig. 12 that high rotating speeds cause leakage peaks for group B. The instantaneous leakage for group B can be increased by up to 600 % when compared with that for group A at the same speeds. This can be explained by the fact that the large additional cylinder block tilting moment due to the piston-slipper assembly mass difference significantly disturbs the cylinder block balance at high speeds and thus results in the cylinder block tilting away from the valve plate. As a result, a wedge-shaped oil film forms within the cylinder block/valve plate interface and consequently leads to a considerable leakage increase from this interface.

Considering the destructive effect of the cylinder block's tilting behavior on the pump performance, the maximum speed of the EHA pump prototype for group B only reached 7000 rpm to prevent the pump failure and even accident.

5. Conclusions

The following conclusions can be drawn from this work.

(1) The effect of piston-slipper assembly mass difference on the cylinder block tilt cannot be neglected, especially when the EHA pump operates at high speeds and low discharge pressures. High additional cylinder block tilting moment may lead to cylinder block tilting away from the valve plate and thus a considerable increase in leakage.

(2) According to Eqs. (17), (18) and (19), the total additional tilting moment consists of one additional tilting moment ΔM_{T1} and another one ΔM_{T2}. Also, ΔM_{T1} dominates the total additional tilting moment.

(3) A tighter control over the piston-slipper assembly mass difference should be achieved for high-speed EHA pumps to avoid cylinder block tilting away from the valve plate and thus increased leakage.

ACKNOWLEDGEMENT

This work was supported by the National Basic Research Program of China (973 Program) (No. 2014CB046403) and the National Natural Science Foundation of China (No. U1509204).

REFERENCES

1. Crowder, R., and Maxwell, C., "Simulation of a prototype electrically powered integrated actuator for civil aircraft," Proceedings of the Institution of Mechanical Engineers, Part G: Journal of Aerospace Engineering, Vol. 211, No. 6, pp. 381-394, 1997.
2. Van Den Bossche, D., "The A380 flight control electrohydrostatic actuators, achievements and lessons learnt," 25TH International Congress of the Aeronautical Sciences, 2006.
3. Navarro, R., "Performance of an electro-hydrostatic actuator on the F-18 systems research aircraft," 16th Digital Avionics Systems Conference, 1997.
4. Chakraborty, I., Mavris, D. N., Emeneth, M., and Schneegans, A., "A methodology for vehicle and mission level comparison of More Electric Aircraft subsystem solution: Application to the flight control actuation system," Proceedings of the Institution of Mechanical Engineers, Part G: Journal of Aerospace Engineering, p. 0954410014544303, 2014.
5. Crowder, R. M., "Electrically powered actuation for civil aircraft," IEE Colloquium on Actuator Technology: Current Practice and New Developments (Digest No: 1996/110), 1996.
6. Edge, K. A., and Darling, J., "The pumping dynamics of swash plate piston pumps," Journal of Dynamic Systems, Measurement, and Control, Vol. 111, No. 2, pp. 307-312, 1989.
7. Carsten, F. B., Lü, X. J., and Stanislav, S., "Pressure compensator (PC) pressure overshoot analysis and experimental research of an open circuit pump," Proceedings of the 2015 International Conference on Fluid Power and Mechatronics, pp. 910-913, 2015.
8. Harris, R. M., Edge, K. A., and Tilley, D. G., "The suction dynamics of positive displacement axial piston pumps," Journal of Dynamic Systems, Measurement, and Control, Vol. 116, No. 2, pp. 281-287, 1994.
9. Yamaguchi, A., and Takabe, T., "Cavitation in an axial piston pump," Bulletin of JSME, Vol. 26, No. 211, pp. 72-78, 1983.
10. Manring, N. D., Mehta, V. S., Nelson, B. E., Graf, K. J., and Kuehn, J. L., "Scaling the speed limitations for axial-piston swash-plate type hydrostatic machines," Journal of Dynamic Systems, Measurement, and Control, Vol. 136, No. 3, p. 031004, 2014.
11. Hong, Y. S., and Kwon, Y. C., "Investigation of the power losses from hydrostatic piston shoe bearings for swash plate type axial piston pumps under mixed friction conditions," International Journal of Precision Engineering and Manufacturing, Vol. 15, No. 11, pp. 2327-2333, 2014.
12. Hong, Y. S., Lee, S. R., Kim, J. H., and Lee, S. Y., "Application of a DLC-Coating for improving hydrostatic piston shoe bearing performance under mixed friction conditions," International Journal of Precision Engineering and Manufacturing, Vol. 16, No. 2, 335-341, 2015.
13. Hong, Y. S., and Doh, Y. H., "Analysis on the friction losses of a bent-axis type hydraulic piston pump," KSME International Journal, Vol. 18, No. 9, pp. 1668-1679, 2004.
14. Lee, S. Y., Kim, S. D., and Hong, Y. S., "Application of the duplex TiN coatings to improve the tribological properties of electro hydrostatic actuator pump parts," Surface and Coatings Technology, Vol. 193, No. 1, 266-271, 2005.
15. Rahmfeld, R., Marsch, S., Göllner, W., Lang, T., Dopichay, T., and Untch, J., "Efficiency potential of dry case operation for bent-axis motors," Proceedings of the 8th International Fluid Power Conference Dresden "fluid power drives", pp. 73-86, 2012.
16. Theissen, H., Gels, S., and Murrenhoff, H., "Reducing energy losses in hydraulic pumps," International Conference on Fluid Power Transmission and Control-ICFP, 2013.
17. Xu, B., Zhang, J. H., Li, Y., and Chao, Q., "Modeling and analysis of the churning losses characteristics of swash plate axial piston pump," Proceedings of the 2015 International Conference on Fluid Power and Mechatronics, pp. 22-26, 2015.
18. Hook, C. J., Kakoullis, Y. P., "The effect of centrifugal load and ball friction on the lubrication of slippers in axial piston pumps," Proceedings of the 6th International Fluid Power Symposium, pp. 179-191, 1981.
19. Hooke, C. J., and Li, K. Y., "The lubrication of slippers in axial piston pumps and motors—the effect of tilting couples," Proceedings of the Institution of Mechanical Engineers, Part C: Journal of Mechanical Engineering Science, Vol. 203, No. 5, pp. 343-350, 1989.
20. Manring, N. D., "Tipping the cylinder block of an axial-piston swash-plate type hydrostatic machine," Journal of Dynamic Systems, Measurement, and Control, Vol. 122, No. 1, pp. 216-221, 2000.
21. Bergada, J. M., Haynes, J. M., and Watton, J., "Leakage and groove pressure of an axial piston pump slipper with multiple lands," Tribology Transactions, Vol. 51, No. 4, pp. 469-482, 2008.
22. Bergada, J. M., Watton, J., Haynes, J. M., and Davies, D. L., "The hydrostatic/hydrodynamic behaviour of an axial piston pump slipper with multiple lands," Meccanica, Vol. 45, No. 4, pp. 585-602, 2010.
23. Bergada, J. M., Kumar, S., Davies, D. L., and Watton, J., "A complete analysis of axial piston pump leakage and output flow ripples," Applied Mathematical Modelling, Vol. 36, No. 4, pp.

1731-1751, 2012.

24. Yamaguchi, A., Sekine, H., Shimizu, S., and Ishida, S., “Bearing/seal characteristics of the film between a valve plate and a cylinder block of axial piston pumps: Effects of fluid types and theoretical discussion,” The Journal of Fluid Control, Vol. 20, No. 4, pp. 7-29, 1990.
25. Greenwood D. T., “Principles of dynamics,” Prentice-Hall, pp. 49-51, 1988.
26. Manring, N. D., “Fluid Power Pumps and Motors: Analysis, Design and Control,” McGraw Hill Professional, pp. 64-66, 2013.
27. Kim, J. K., and Jung, J. Y., “Measurement of fluid film thickness on the valve plate in oil hydraulic axial piston pumps (I)-bearing pad effects,” KSME International Journal, Vol. 17, No. 2, pp. 246-253, 2003.
28. Kim, J. K., Kim, H. E., Lee, Y. B., Jung, J. Y., and Oh, S. H., “Measurement of fluid film thickness on the valve plate in oil hydraulic axial piston pumps (Part II: Spherical design effects),” Journal of Mechanical Science and Technology, Vol. 19, No. 2, pp. 655-663, 2005.
29. Deeken, M., “Simulation of the tribological contacts in an axial piston machine,” Proceedings of ASME 2004 International Mechanical Engineering Congress and Exposition, pp. 71-75, 2004.
30. Wieczorek, U., and Ivantysynova, M., “Computer aided optimization of bearing and sealing gaps in hydrostatic machines—the simulation tool CASPAR,” International Journal of Fluid Power, Vol. 3, No. 1, pp. 7-20, 2002.
31. Bergada, J. M., Davies, D. L., Kumar, S., and Watton, J., “The effect of oil pressure and temperature on barrel film thickness and barrel dynamics of an axial piston pump,” Meccanica, Vol. 47, No. 3, pp. 639-654, 2012.
32. Zhai, P. X., “The design of swash-plate axial piston pump,” Coal Industry Press, pp. 77-81, 1978.
33. Kulshreshtha, A., and Charrier, J., “Electric actuation for flight and engine control: evolution and challenges,” SAE-ACGSC Meeting, Vol. 99, 2007.